VIII. On Creep Failure of Balloons

Arnold D. Kerr
Department of Aeronautics and Astronautics
New York University
University Heights, New York

Abstract

Assuming that the balloon material responds like a Maxwell model, it is demonstrated that there exists a critical time at which the balloon will rupture. The characteristic features of this phenomenon are demonstrated on a spherical balloon which is subjected to a constant internal pressure, with no restrictions imposed upon the magnitude of the balloon displacements. Planned investigations to correlate these phenomena of creep failure with recent balloon failures are outlined.

1. INTRODUCTION AND STATEMENT OF PROBLEM

In recent years increasing demands on balloons, such as heavier payloads and higher altitudes, have necessitated a rapid development of balloon technology. A significant step in this direction was the introduction of newly developed thin plastic films (polyethylene, mylar, etc.) as balloon materials. Because of their light weight and relative strength, a 10,000,000 cu ft balloon that can lift 150 lb to an altitude of 150,000 ft is not unusual.

This development is accompanied, however, by an increasing number of balloon failures. Studying the available records of numerous balloon flights conducted by AFCRL and NCAR, one finds that a large number of the balloons that failed did so at altitudes between 40,000 and 60,000 ft. Possible causes of failure are the phenomena associated with the creep deformations of the balloon skin which occur during balloon launch and ascent, as well as changes in the material's properties caused by the temperature of the atmosphere through which the balloon passes. A typical temperature profile is shown in Figure 1. It should be noted that the temperature difference between launch and that at 45,000 ft can be as much as 120°F.

Movie cameras mounted inside of balloons recorded some of the failures, revealing that they occurred in the upper part of the balloon where the skin was taut. This finding, and the fact that the upper part of an inflated balloon, in addition to being stressed biaxially, is often subjected to intense solar heating, suggest as a first step studying the possibility of failure caused by creep deformations.

Kac (1957), Kachanov (1958, 1960), Finnie (1959), Rimrott (1959), Rimrott et al (1960), and Odquist and Hult (1962) considered the problem of rupture of metallic pressure vessels at high temperatures caused by large creep deformations. Because of the mechanical properties of metals it seemed justified to neglect the relatively small elastic deformations. Problems involving tension instability of elastic materials subjected to large deformations are treated by Rzhanitzyn (1955), Panovko and Gubanova (1964) and Levinson (1965).

The following presentation, a generalization of the analyses in Rzhanitzyn (1965) and Panovko and Gubanova (1964), assumes that the balloon material responds like a viscoelastic body. Since for a number of balloon materials the elastic deformations may be very large, they are retained in the analysis. In view of the present lack of experimental data for the balloon materials in question, it is assumed that the material is incompressible and that it responds to deviatoric deformations like a Maxwell body when formulation is in terms of true stresses and logarithmic strains.

The creep failure phenomenon preceded by large elastic deformations is studied first on a thin strip subjected to tension and then on a spherical balloon subjected to a uniform internal pressure.

2. THE THIN STRIP SUBJECTED TO UNIAXIAL TENSION

We consider a thin homogeneous and isotropic strip subjected uniaxially to a force P as shown in Figure 2. The area of the initial cross section is $A_o = b_o h_o$. It is assumed that the area of the deformed cross section after the load P is applied is $A = bh$. L_o is the initial length of strip under consideration and L the length after deformation. The rate of application of P and the expected rates of deformation of the strip are assumed to be very small, so that inertia terms are negligible.

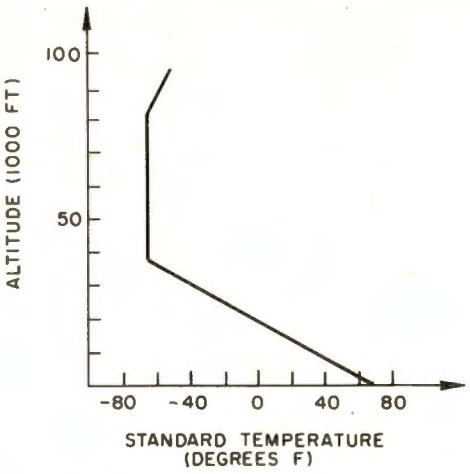

Figure 1. Atmospheric Height-Temperature Profile

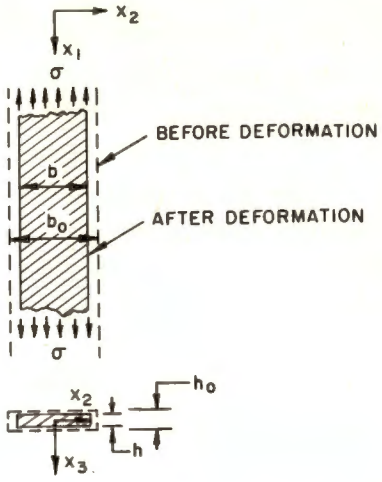

Figure 2. Thin Strip Subjected to Uniaxial Force

The equilibrium equation of the strip at a certain instant after the load is applied is

$$\sigma A = P . \tag{1}$$

The kinematic relations are

$$\epsilon_{11} = \ln\left(\frac{L}{L_o}\right) \tag{2}$$

$$\epsilon_{22} = \ln\left(\frac{b}{b_o}\right) \tag{3}$$

$$\epsilon_{33} = \ln\left(\frac{h}{h_o}\right) . \tag{4}$$

Since the strip material is assumed incompressible, the geometrical quantities are interrelated by the equation

$$A_o L_o = AL . \tag{5}$$

With Eq. (5), ϵ_{11} may be expressed as

$$\epsilon_{11} = \ln\left(\frac{b_o h_o}{bh}\right) . \tag{6}$$

It can be easily verified that because of Eq. (5)

$$\epsilon_{11} + \epsilon_{22} + \epsilon_{33} = 0 \, . \tag{7}$$

We treat first the elastic case, which occurs at the instant of loading (t = 0). We assume as constitutive equations Hooke's law for true stresses and logarithmic strains

$$\left.\begin{aligned} \epsilon_{11} &= \frac{1}{E}\left\{\sigma_{11} - \nu\,(\sigma_{22} + \sigma_{33})\right\} \\ \epsilon_{22} &= \frac{1}{E}\left\{\sigma_{22} - \nu\,(\sigma_{11} + \sigma_{33})\right\} \\ \epsilon_{33} &= \frac{1}{E}\left\{\sigma_{33} - \nu\,(\sigma_{11} + \sigma_{22})\right\} \end{aligned}\right\} \tag{8}$$

The effect of deformational anisotropy (Berg, 1958) is not taken into consideration in the present analysis. Since the material is incompressible, $\nu = 1/2$. Noting that

$$\epsilon_{11} = \sigma \quad \text{and} \quad \sigma_{22} = \sigma_{33} = 0 \, ,$$

Eq. (8) reduce to

$$\epsilon_{11} = \frac{\sigma}{E} \tag{9}$$

and

$$\epsilon_{22} = \epsilon_{33} = -\frac{\sigma}{2E} \, . \tag{10}$$

Because of Eq. (7), only one of the three equations given in Eqs. (9) and (10) is independent. Elimination of ϵ_{11} from Eqs. (2) and (9) results in

$$\sigma = E \, \ln\left(\frac{L_{el}}{L_o}\right) . \tag{11}$$

Substitution of Eq. (11) into the equilibrium Eq. (1), noting Eq. (5), yields

$$\boxed{\epsilon_o = \frac{1}{L^*_{e1}} \ln L^*_{el}} \tag{12}$$

where

$$\epsilon_o = \frac{P}{EA_o} = \frac{\sigma_o}{E} \tag{13}$$

$$L^*_{el} = \frac{L_{e1}}{L_o} .$$

The graphical representation of Eq. (12) is shown in Figure 3. The maximum value of ϵ_o is obtained from the condition $d\epsilon_o/dL^*_{el} = 0$. It is

$$\epsilon_{o,\max} = \frac{1}{e} \tag{14}$$

and takes place at

$$L^*_{el} = e . \tag{15}$$

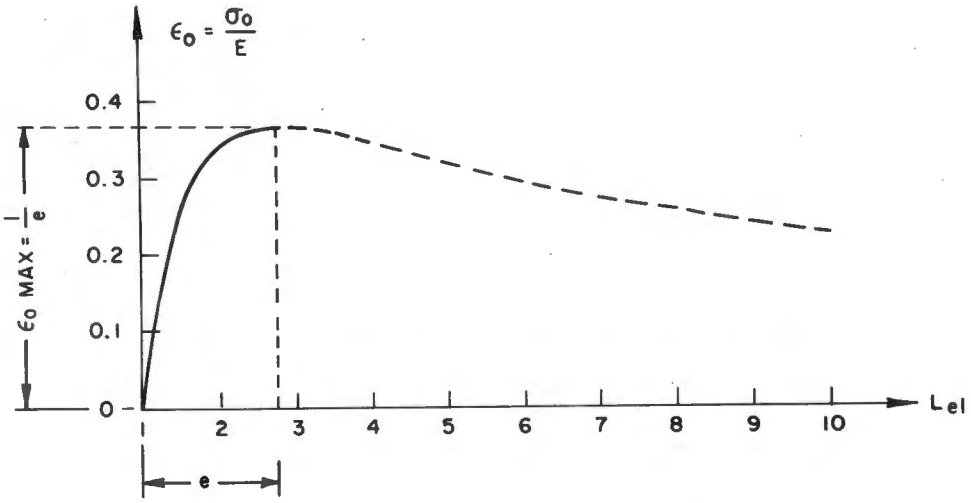

Figure 3. Graph of ϵ_o Versus L^*_{el}

Thus, elastic tensile instability takes place at

$$L_{el} \approx 2.7 L_o . \tag{16}$$

In a real situation the strip may contain material imperfections that can weaken the strip locally. Another possibility is that at some place along the strip the area of the initial cross section, A_o, may be smaller than those along the remaining parts of the strip. In such instances the weaker or smaller cross section will determine the possible maximum value of ϵ_o and the corresponding large deformations will be restricted to this region. This argument was presented by N. J. Hoff (1953) to explain the initiation of necking in a tensile specimen.

For the analysis of the viscoelastic response, it is often convenient to split the stress and stain tensor into a deviatoric and volumetric part and then prescribe separate constitutive equations for the deviatoric and volumetric response (Lee, 1958). For example, an equivalent form of Hooke's law presented by Kachanov (1960) is

$$s_{ij} = 2 \mu e_{ij} \tag{17}$$

$$\sigma_{kk} = 3K\epsilon_{kk} \tag{18}$$

where σ_{ij} are the components of the stress tensor
s_{ij} are the components of the stress deviator
ϵ_{ij} are the components of the strain tensor
e_{ij} are the components of the strain deviator
and s_{ij} and e_{ij} are defined as follows:

$$s_{ij} = \sigma_{ij} - \frac{1}{3}\delta_{ij}\sigma_{kk} \tag{19}$$

$$e_{ij} = \epsilon_{ij} - \frac{1}{3}\delta_{ij}\epsilon_{kk} \tag{20}$$

where

$$\sigma_{kk} = \sigma_{11} + \sigma_{22} + \sigma_{33} \tag{21}$$

$$\epsilon_{kk} = \epsilon_{11} + \epsilon_{22} + \epsilon_{33} . \tag{22}$$

The new elastic constants μ and K are related to E and ν as follows:

$$\mu = \frac{E}{2(1+\nu)} \quad ; \quad K = \frac{E}{3(1-2\nu)} \ . \tag{23}$$

For an incompressible material

$$K = \infty \text{ and } \mu = \frac{E}{3} \ . \tag{24}$$

Because of the assumed incompressibility of the material, the constitutive equations are

$$s_{ij} = 2\mu\epsilon_{ij} \ . \tag{25}$$

The strip problem treated above may be solved by using the new form for the constitutive equations, as follows:

We decompose the stress tensor in accordance with Eq. (19)

$$\begin{bmatrix} \sigma & 0 & 0 \\ 0 & 0 & 0 \\ 0 & 0 & 0 \end{bmatrix} = \begin{bmatrix} \frac{\sigma}{3} & 0 & 0 \\ 0 & \frac{\sigma}{3} & 0 \\ 0 & 0 & \frac{\sigma}{3} \end{bmatrix} + \begin{bmatrix} \frac{2}{3}\sigma & 0 & 0 \\ 0 & -\frac{1}{3}\sigma & 0 \\ 0 & 0 & -\frac{1}{3}\sigma \end{bmatrix} \tag{26}$$

and thus obtain

$$\left.\begin{aligned} s_{11} &= \frac{2}{3}\sigma \quad ; \quad s_{22} = s_{33} = -\frac{1}{3}\sigma \\ s_{ij} &= 0 \quad \text{for } i \neq j \end{aligned}\right\} \tag{27}$$

With Eq. (27), the constitutive equations, Eq. (25), assume the form

$$\left.\begin{aligned} \frac{2}{3}\sigma &= 2\mu \ \ln\left(\frac{L_{el}}{L_o}\right. \\ -\frac{1}{3}\sigma &= 2\mu \ \ln\left(\frac{b_{el}}{b_o}\right) \\ -\frac{1}{3}\sigma &= 2\mu \ \ln\left(\frac{h_{el}}{h_o}\right) \ . \end{aligned}\right\} \tag{28}$$

Noting Eq. (5), it can be easily shown that only one constitutive equation is independent. Substitution of the first equation into the equilibrium Eq. (1) yields, considering Eqs. (5) and (24), Eq. (12).

Figure 4. Maxwell Body

We proceed now to solve the viscoelastic case, that is, behavior of the strip for $t>0$. We retain the assumption that the material is incompressible, and assume that it responds to deviatoric deformations like a Maxwell body (see Figure 4). The corresponding constitutive equations are (see Hilton, 1962), noting that $e_{ij} = e_{ij}$,

$$\left(\frac{d}{dt} + \frac{\mu}{\eta}\right)s_{ij} = 2\mu\frac{d\epsilon_{ij}}{dt} \quad . \tag{29}$$

With the s_{ij} values given in Eq. (27) and the ϵ_{ij} in Eqs. (2), (3), and (4), the constitutive equations become

$$\frac{2}{3}\left(\frac{d}{dt} + \frac{\mu}{\eta}\right)\sigma = 2\mu\,\frac{d}{dt}\left(\ln\frac{L}{L_o}\right) \tag{30}$$

$$-\frac{1}{3}\left(\frac{d}{dt} + \frac{\mu}{\eta}\right)\sigma = 2\mu\,\frac{d}{dt}\left(\ln\frac{b}{b_o}\right) \tag{31}$$

$$-\frac{1}{3}\left(\frac{d}{dt} + \frac{\mu}{\eta}\right)\sigma = 2\mu\,\frac{d}{dt}\left(\ln\frac{h}{h_o}\right) \tag{32}$$

where σ, L, b, and h are functions of time and $P = \sigma(t)A(t) = \text{const}$. Because of Eq. (5), only one of Eqs. (30), (31), and (32) is independent.

Combining the equilibrium Eq. (1), valid at a time instant t, with the incompressibility condition, Eq. (5), we obtain

$$\sigma(t) = \frac{PL(t)}{A_o L_o} \quad . \tag{33}$$

Substituting Eq. (33) into Eq. (30) we obtain, setting

$$\frac{L}{L_o} = L^*(t) \qquad \sigma_o = \frac{P}{A_o} \quad , \tag{34}$$

the equation

$$\sigma_o\left(\frac{d}{dt}+\frac{\mu}{\eta}\right)L^* = 3\mu\frac{d}{dt}(\ln L^*)\ . \tag{35}$$

Noting that

$$\frac{d}{dt}(\ln L^*) = \frac{1}{L^*}\frac{dL^*}{dt}\ , \tag{36}$$

the equation describing the problem assumes the form

$$\left[\frac{3\mu - \sigma_o L^*}{L^*}\right]\frac{dL^*}{dt} = \sigma_o\frac{\mu}{\eta}L^*\ . \tag{37}$$

This is a first-order, nonlinear, ordinary differential equation with separable variables. Integrating it directly

$$\int_{L^*=L^*_{el}}^{L^*}\left(\frac{3\mu}{L^{*2}e}-\frac{\sigma_o}{L^*}\right)dL^* = \sigma_o\frac{\mu}{\eta}\int_{t=0}^{t}dt\ , \tag{38}$$

we obtain the solution

$$\boxed{\frac{1}{\epsilon_o}\left[\frac{1}{L^*_{el}}-\frac{1}{L^*}\right]-\ln\left(\frac{L^*}{L^*_{el}}\right)=t^*} \tag{39}$$

where

$$\epsilon_o = \frac{\sigma_o}{3\mu} = \frac{P}{3\mu A_o}\ ; \qquad t^* = \frac{\mu}{\eta}t\ . \tag{40}$$

In order to study how the deformations vary with time, L^* - t^* graphs for various values of ϵ_o are constructed.

For this purpose we assume values of $\epsilon_o < \epsilon_{o,max}$ and obtain from Figure 3 the corresponding L^*_{el} values. Each pair (ϵ_o, L^*_{el}), which constitutes an initial condition for a given load P, is then substituted into Eq. (39), which is then numerically evaluated. The results are shown in Figure 5.

It can be seen that for each $\epsilon_o < \epsilon_{o,max}$ there is a critical time at which the strip will fail, and that these time intervals increase with decreasing values of

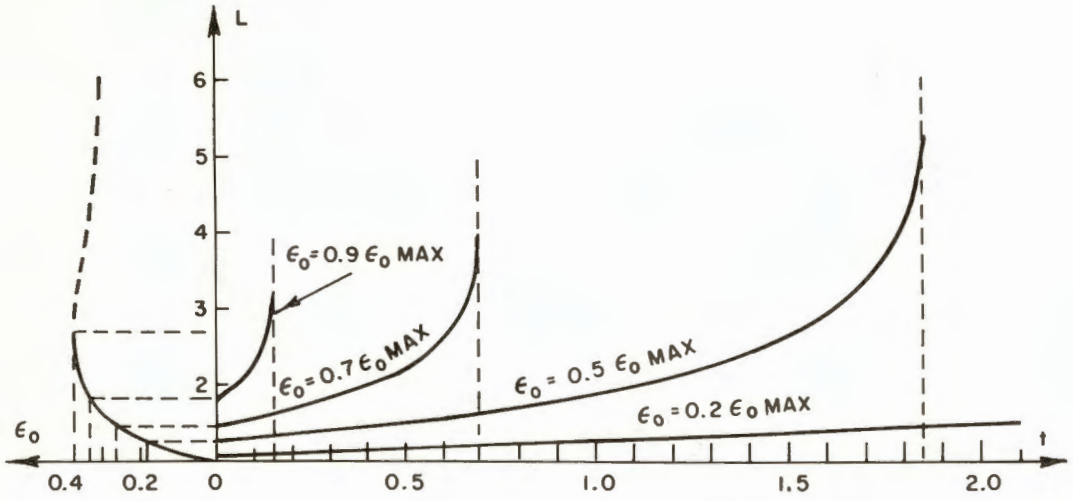

Figure 5. Graph of L^* Versus t^*

$\epsilon_o < \epsilon_{o,max}$. For $\epsilon_o = \epsilon_{o,max}$ the critical time is zero. Analytically the values for the critical time may be determined using the condition $\frac{\partial t^*}{\partial L^*} = 0$. They are

$$t_{crit} = \frac{\eta}{\mu}\left[\frac{1}{\epsilon_o L^*_{el}} + \ln(\epsilon_o L^*_{el}) - 1\right] \tag{41}$$

Where the strip contains locally a material imperfection or a smaller cross section, as discussed before, the creep deformations will also be larger and the strip will finally fail. The critical time will be governed by the properties of this local region (Hoff, 1953).

3. THE SPHERICAL BALLOON SUBJECTED TO A CONSTANT INTERNAL PRESSURE

We consider a thin spherical balloon subjected to a uniform internal pressure p_o. It is assumed that p_o is maintained constant during the creep deformation process. In the present case the true stresses increase more rapidly than in the case of the strip discussed before, since in addition to the decrease of the skin thickness the total force acting on

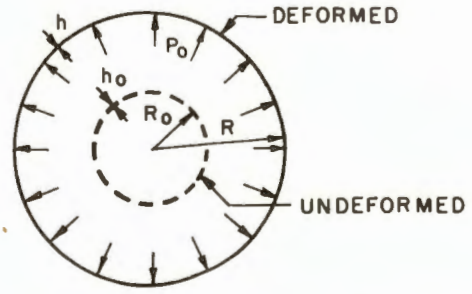

Figure 6. Thin Spherical Balloon Subjected to Pressure p_o

the sphere increases with time because of the increase of the balloon diameter. The situation to be analyzed is shown in Figure 6. R_o is the radius of the middle surface of the undeformed balloon, and h_o is the skin thickness. R and h are the respective dimensions of the deformed balloon at the instant of consideration.

It is assumed that: (1) the material is homogeneous and isotropic and retains its spherical shape during deformation; (2) $h_o \ll R_o$ and $h \ll R$; (3) the balloon skin behaves like a membrane, that is, $\sigma_{\phi\phi}$ and $\sigma_{\theta\theta}$ are uniformly distributed across the skin and σ_{rr} is negligibly small compared to $\sigma_{\phi\phi}$ and $\sigma_{\theta\theta}$; and (4) the rate of application of p_o and the expected rates of deformation of the spherical membrane are small, so that inertia terms are negligible.

The equilibrium condition on a part of the deformed balloon yields

$$\sigma = \frac{p_o R}{2h} \tag{42}$$

where σ is the true membrane stress.

The kinematic relations are*

$$\epsilon_{\theta\theta} = \epsilon_{\phi\phi} = \ln\left(\frac{R}{R_o}\right) = \epsilon \tag{43}$$

$$\epsilon_{rr} = \ln\left(\frac{h}{h_o}\right). \tag{44}$$

The incompressibility condition

$$\frac{4}{3}\pi\left[\left(R + \frac{h}{2}\right)^3 - \left(R - \frac{h}{2}\right)^3\right] = \frac{4}{3}\pi\left[\left(R_o + \frac{h_o}{2}\right)^3 - \left(R_o - \frac{h_o}{2}\right)^3\right] \tag{45}$$

reduces, after expansion, to

$$\left[\left(\frac{h}{2}\right)^3 + 3R^2\frac{h}{2}\right] = \left[\left(\frac{h_o}{2}\right)^3 + 3R_o^2\frac{h_o}{2}\right]. \tag{46}$$

Neglecting the first terms on both sides of Eq. (46) as being small (of higher order) compared to the remaining ones, we obtain the equation

$$R^2 h = R_o^2 h_o \tag{47}$$

---

* In deriving Eq. (44) it is assumed, because of the thinness of the membrane, that ϵ_{rr} is constant throughout the balloon skin.

which will be used as the incompressibility condition in the following analysis. Because of Eq. (47), we may rewrite Eq. (44) as

$$\epsilon_{rr} = -\,2\,\ln\left(\frac{R}{R_o}\right) . \tag{48}$$

We consider first the elastic case which takes place at the instant of loading (t = 0) and assume as constitutive equations

$$s_{ij} = 2\mu\epsilon_{ij} \qquad (i,j = r,\ \theta,\ \phi) . \tag{25}$$

We decompose the stress tensor in accordance with Eq. (19)

$$\begin{bmatrix} 0 & 0 & 0 \\ 0 & \sigma & 0 \\ 0 & 0 & \sigma \end{bmatrix} = \begin{bmatrix} \frac{2}{3}\sigma & 0 & 0 \\ 0 & \frac{2}{3}\sigma & 0 \\ 0 & 0 & \frac{2}{3}\sigma \end{bmatrix} + \begin{bmatrix} -\frac{2}{3}\sigma & 0 & 0 \\ 0 & \frac{1}{3}\sigma & 0 \\ 0 & 0 & \frac{1}{3}\sigma \end{bmatrix} \tag{49}$$

and thus obtain

$$\begin{aligned} &s_{rr} = -\frac{2}{3}\sigma\ ; \quad s_{\theta\theta} = \frac{1}{3}\sigma \quad ; \quad s_{\phi\phi} = \frac{1}{3}\sigma \\ &s_{ij} = 0 \quad \text{for} \quad i \neq j . \end{aligned} \tag{50}$$

The only independent constitutive equation which remains after substituting Eqs. (50), (43) and (48) into Eq. (25) is

$$\sigma = 6\mu\ \ln\left(\frac{R_{el}}{R_o}\right) . \tag{51}$$

Substituting Eq. (51) into Eq. (42) and noting Eq. (47), we obtain

$$\boxed{\epsilon_o = \frac{1}{R_{el}^{*3}}\ \ln R_{el}^*} \tag{52}$$

where

$$\epsilon_o = \frac{p_o R_o}{12\mu h_o} = \frac{\sigma_o}{6\mu} \qquad R_{el}^* = \frac{R_{el}}{R_o} . \tag{53}$$

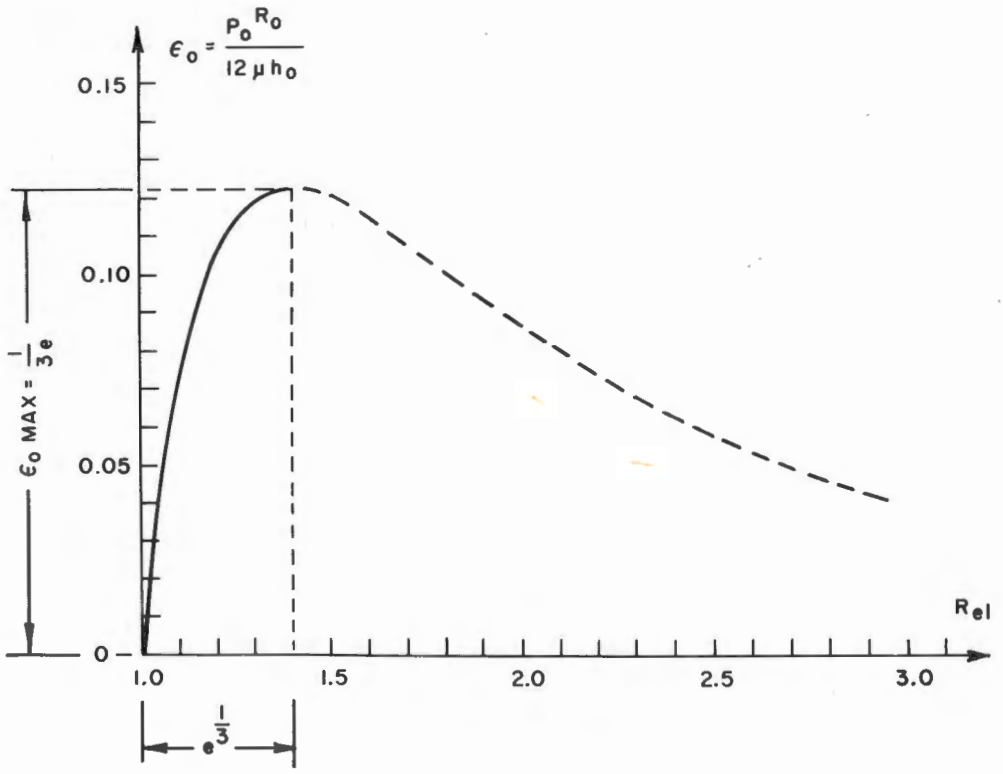

Figure 7. Graph of ϵ_o Versus R_{el}^*

The graphical representation of Eq. (52) is shown in Figure 7. The maximum value of ϵ_o is obtained from the condition $d\epsilon_o/dR_{el}^* = 0$. It is

$$\epsilon_{o,max} = \frac{1}{3e} \tag{54}$$

and takes place at

$$R_{el}^* = e^{1/3} . \tag{55}$$

Thus the elastic tensile instability takes place at

$$R_{el} \approx 1.4 R_o . \tag{56}$$

In a real situation the balloon skin may contain along a line or curve, or inside of a small region, imperfections of a physical or geometrical nature which will

weaken locally the balloon skin. Such regions will significantly affect the value of p_o. Large deformations as well as rupture are expected to take place in such regions.

For the viscoelastic analysis we retain, as before, the assumption that the material is incompressible and that it responds to deviatoric deformations like a Maxwell body. Thus the general form of the constitutive equations are given in Eq. (29). Substituting into Eq. (29) the σ_{ij}'s given in Eq. (50) and the ϵ_{ij}'s given in Eqs. (43) and (48), we obtain for the problem under consideration the constitutive equation

$$\left(\frac{d}{dt} + \frac{\mu}{\eta}\right)\sigma = 6\mu \frac{d}{dt} \ln\left(\frac{R}{R_o}\right) \tag{57}$$

where $\sigma = \sigma(t)$ and $R = R(t)$.

The equilibrium equation at a time t is given in Eq. (42). Noting the incompressibility condition, Eq. (47), Eq. (42) assumes the form

$$\sigma = \frac{p_o R^{*3}}{2h_o^*} \tag{58}$$

where

$$R^* = \frac{R}{R_o} \quad ; \qquad h_o^* = \frac{h_o}{R_o} \, . \tag{59}$$

In the following analysis it is assumed that for $t \geq 0$ the pressure p_o is maintained constant. Substitution of Eq. (58) into Eq. (57) yields

$$\left[\frac{3\,p_o}{2\,h_o^*} R^{*3} - 6\mu\right] \frac{dR^*}{dt} + \frac{\mu p_o}{2\eta h_o^*} R^{*4} = 0 \, . \tag{60}$$

This is a first-order, nonlinear, ordinary differential equation with separable variables that can be integrated directly as follows:

$$\int_{R^*=R_{el}^*}^{R^*} \left[\frac{3p_o/2h_o^*}{R^*} - \frac{6\mu}{R^{*4}}\right] dR^* = -\frac{\mu p_o}{2\eta h_o^*} \int_{t=0}^{t} dt \, . \tag{61}$$

Performing the integrations we obtain the solution

$$\boxed{\frac{1}{3\epsilon_o}\left[\frac{1}{R^{*3}_{el}} - \frac{1}{R^{*3}}\right] - 3\ln\left(\frac{R^*}{R^*_{el}}\right) = t^*} \tag{62}$$

where

$$t^* = \frac{\mu}{\eta} t \,. \tag{63}$$

The R^* - t^* graphs are constructed in a similar manner as the L^* - t^* graphs for the strip, and they are shown in Figure 8. The corresponding values for the critical time are

$$\boxed{t_{crit} = \frac{\eta}{\mu}\left[\frac{1}{(3\epsilon_o R^{*3}_{el})} + \ln(3\epsilon_o R^{*3}_{el}) - 1\right]} \tag{64}$$

Hence for a balloon skin material obeying the constitutive equations given in Eq. (57) for a given value of the internal pressure p_o, the instantaneous elastic deformations may be determined from Eq. (52) or Figure 7. The critical time can then be determined directly from Eq. (64).

From Figure 8 it can be seen that the balloon deformations due to creep increase slowly at the beginning but increase very rapidly as the time approaches

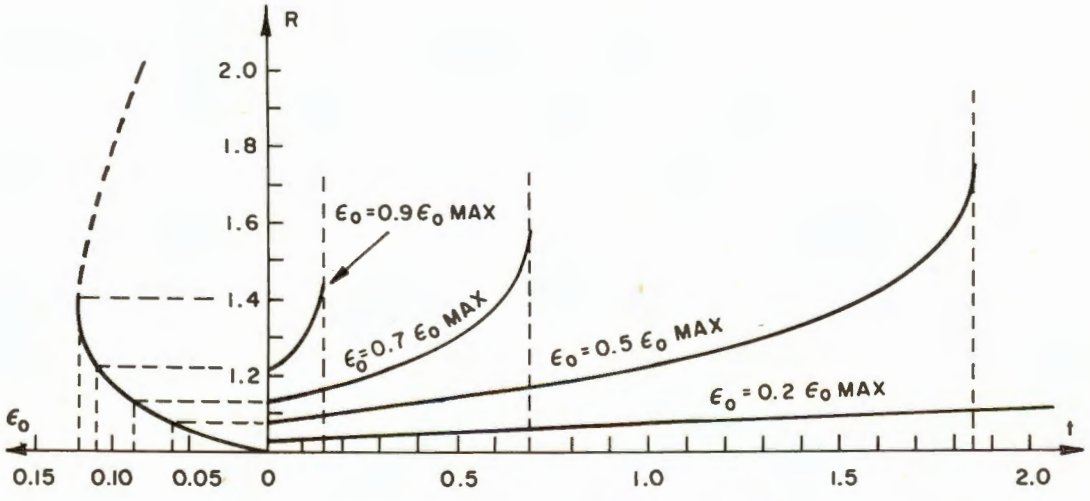

Figure 8. Graph of R^* Versus t^*

t_{crit}. Since the skin thickness diminishes and the radius increases for $t > 0$ and p_o maintained constant, it is expected that in the later phase of the deformations the true stresses will reach a level where brittle fracture or plastic deformations will take place and thus the real rupture time will be smaller that t_{crit} (Carlson, 1964).

At this stage it should be recalled that the above derivations are based on the assumptions that the balloon material is incompressible and that it responds to deviatoric deformations like a linear Maxwell body when formulation is in terms of true stresses and logarithmic strains. Also the effect of deformational anisotropy was not taken into consideration, which for polymers may be very pronounced for certain types of deformations. For these reasons the above derivations and presented results should be considered, at the present, more of an expository nature. Tests are presently being conducted on a number of balloon materials currently in use (rubbers and polymers) which should clarify these issues and yield constitutive equations for each of the materials in question. The constitutive equations for each material will then be used to determine deformations and rupture time for balloons of various shapes. These data will then be compared with corresponding measurements of controlled balloon experiments in an attempt to establish whether creep rupture is the major cause of the described balloon ascent-failures. If confirmed, the developed analytical results and the accumulated data and experience from the experimental program should be very helpful in finding ways to prevent creep failures of balloons.

Acknowledgment

The author wishes to acknowledge the assistance of Mr. Harold Alexander, graduate student, for performing the numerical evaluations presented in the graphs and proofreading the manuscript.

References

Berg, B. A. (1958) Deformational anisotropy, Prikladnaia Matematika i Mekhanika, 22 (No. 1): 67-77.

Carlson, R. L. (1964) An Analysis of Creep Rupture, Presented at the ASME Winter Annual Meeting, Paper Nr. 64-WA/MET-14.

Finnie, I. (1959) A creep instability of thin walled tubes under internal pressure, Journal of Aero/Space Sciences, April, p. 248-249.

Hilton, H. H. (1962) An introduction to Viscoelastic Analysis, Technical Report AAE 62-1, Aeronautical and Astronautical Engineering Department, University of Illinois, Urbana, Illinois.

Hoff, N. J. (1953) The necking and rupture of rods subjected to constant tensile loads, Journal of Applied Mechanics, 20:105-108.

Kac, Sh. N. (1957) Creep and Rupture of Tubes Subjected to Internal Pressure (in Russian), Izvestia, AN USSR, OTN, Nr. 10.

Kachanov, L. M. (1958) On Creep Rupture Time (in Russian), Izvestia AN USSR, OTN, Nr. 8.

Kachanov, L. M. (1960) Theory of Creep (in Russian), Fizmatgiz, Moscow, Section 58.

Lee, E. H. (1958) Viscoelastic Stress Analysis, Proc. of First Symposium on Naval Structural Mechanics, Stanford University.

Levinson, M. (1965) The Application of the principle of stationary potential energy to some problems in finite elasticity, Journal of Applied Mechanics, Sept., pp. 656-660.

Odquist, F. K. G., and Hult, J. (1962) Kriechfestigkeit Metallischer Werkstoffe, Springer-Verlag, Berlin/Göttingen/Heidelberg, Chapter IV.

Panovko, Ja. G., and Bubanova, I. I. (1964) Stability and Vibrations of Elastic Systems (in Russian), Izdatelstvo Nauka, Moscow, Part IV.

Rimrott, F. (1959) Versagenszeit beim Kriechen, Ingenieur Archiv, 27: 169-178.

Rimrott, F. P. J., Mills, E. J., and Marin, J. (1960) Prediction of creep failure time for pressure vessels, Journal of Applied Mechanics, June, p. 303-308.

Rzhanitzyn, A. R. (1955) Stability of Equilibrium of Elastic Systems (in Russian) Gostekhizdat, Moscow, Section 23.